



Polyfluorinated bis-styrylbenzenes as amyloid- β plaque binding ligands



Rob J. A. Nabuurs^{a,*}, Varsha V. Kapoor^{b,†}, Athanasios Metaxas^c, Sanne de Jongh^a, Maaïke de Backer^a, Mick M. Welling^a, Wim Jiskoot^d, Albert D. Windhorst^c, Hermen S. Overkleeft^b, Mark A. van Buchem^a, Mark Overhand^b, Louise van der Weerd^{a,e}

^a Department of Radiology CS2, Leiden University Medical Center, Albinusdreef 2, 2333 ZA Leiden, Netherlands

^b Department of Bioorganic Synthesis, Leiden Institute of Chemistry, Leiden University, Leiden, Netherlands

^c Radionucleotide Laboratory, Free University, Amsterdam, Netherlands

^d Division of Drug Delivery Technology, Leiden Academic Center for Drug Research, Leiden University, Netherlands

^e Department of Human Genetics, Leiden University Medical Center, Leiden, Netherlands

ARTICLE INFO

Article history:

Received 17 October 2013

Revised 25 February 2014

Accepted 28 February 2014

Available online 7 March 2014

Keywords:

Amyloid β

Fluorine

Imaging

Alzheimer's disease

Contrast agent

ABSTRACT

Detection of cerebral β -amyloid ($A\beta$) by targeted contrast agents remains of great interest to aid the in vivo diagnosis of Alzheimer's disease (AD). Bis-styrylbenzenes have been previously reported as potential $A\beta$ imaging agents. To further explore their potency as ^{19}F MRI contrast agents we synthesized several novel fluorinated bis-styrylbenzenes and studied their fluorescent properties and amyloid- β binding characteristics. The compounds showed a high affinity for $A\beta$ plaques on murine and human brain sections. Interestingly, competitive binding experiments demonstrated that they bound to a different binding site than chrysamine G. Despite their high $\log P$ values, many bis-styrylbenzenes were able to enter the brain and label murine amyloid in vivo. Unfortunately initial post-mortem ^{19}F NMR studies showed that these compounds as yet do not warrant further MRI studies due to the reduction of the ^{19}F signal in the environment of the brain.

© 2014 Published by Elsevier Ltd.

1. Introduction

Alzheimer's disease (AD) is the predominant form of dementia in the aging population. The disease is marked by neuronal degeneration associated with deposits of tau proteins in intraneuronal neurofibrillary tangles (NFTs) and of amyloid- β ($A\beta$) peptides in extracellular amyloid plaques.¹ Although the precise role of amyloid in AD pathology is still not completely understood, accumulation of amyloid plaques is thought to precede the onset of the first clinical symptoms by up to two decades.^{2,3} A clinical imaging technique capable of visualizing and quantifying these early changes thus may enable early diagnosis and better understanding of the pathophysiology.

Over the past years progress has been made in the development of $A\beta$ -targeting imaging ligands suitable for visualization by positron emission tomography (PET), single positron emission tomography (SPECT), fluorescence microscopy or magnetic resonance imaging (MRI).

For clinical use, the [^{11}C]-benzothiazole derivative Pittsburgh compound B (PiB, **1**, Fig. 1) is the best characterized in vivo PET radiotracer. However, as the short half-life of ^{11}C limits its use to medical centers with an on-site cyclotron, alternatives are desired. Therefore, several longer-lived ^{18}F radiofluorinated derivatives have been designed, like flutemetamol (**2**),⁴ florbetapir (**3**) and florbetaben(**4**),⁵ of which the first two recently have been the first to be admitted for commercial use with the last one expected to follow soon thereafter.^{6,7} Despite the inherent high sensitivity of PET, the development of $A\beta$ -targeted imaging probes suitable for clinical MRI remains attractive as this would lower the threshold for performing amyloid scans given the wider availability of MRI systems as compared to PET systems, the lack of ionizing irradiation and the lower costs involved in performing clinical MRI as compared to PET. Furthermore, such agents could be used in one scan session comprising a comprehensive structural and functional scan protocol as well as a scan to detect the molecular imaging tracers, whereas one PET examination only provides one biomarker.

Based on congo red (**5**), several bis-styrylbenzenes have been reported to show strong $A\beta$ binding affinities and serve as potential backbones for in vivo PET or SPECT imaging probes, like **6** (chrysamine G), **7** (X-34),⁸ **8** (ISB)⁹ and **10** (Methoxy-X04)¹⁰ (Fig. 1 and Scheme 1). The styrylbenzene backbone has also been explored

* Corresponding author. Tel.: +31 71 526 4376.

E-mail address: r.j.a.nabuurs@lumc.nl (R.J.A. Nabuurs).

† Authors have contributed to this work equally.

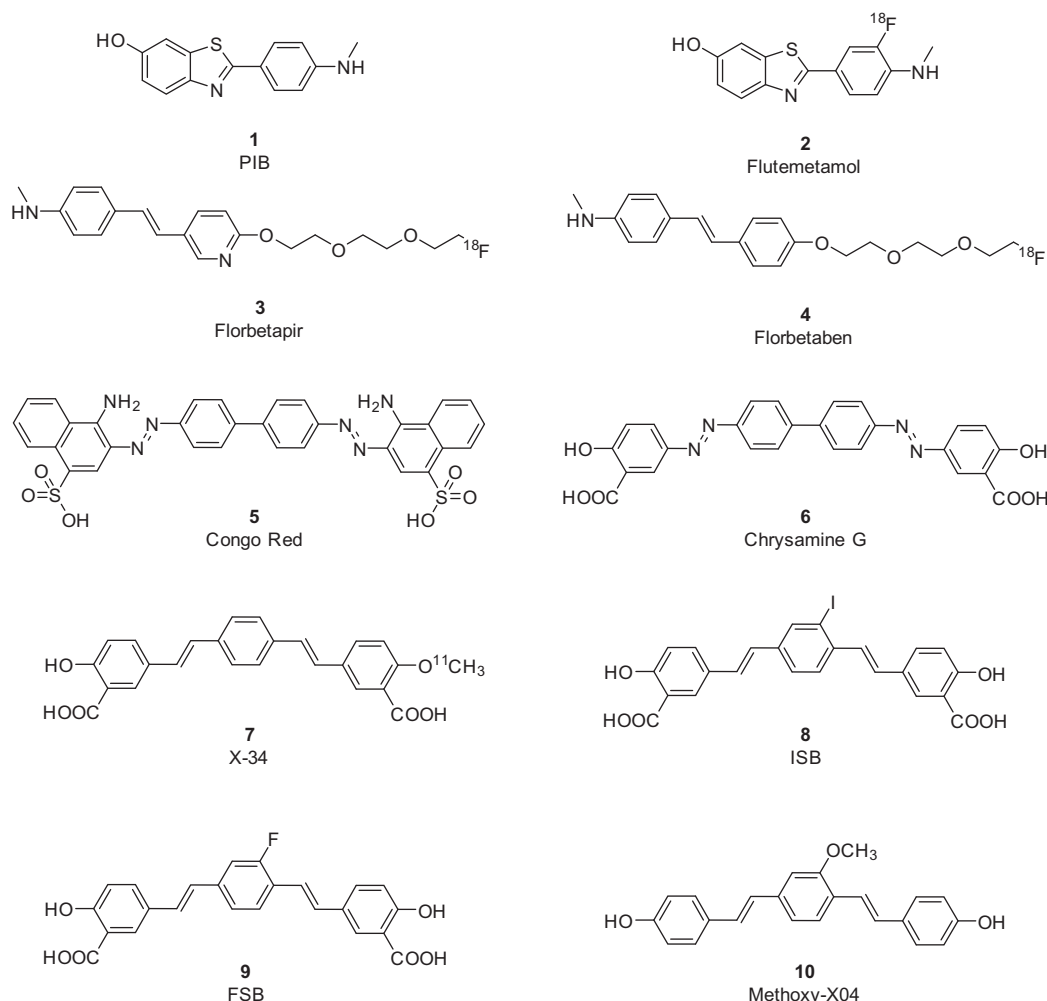


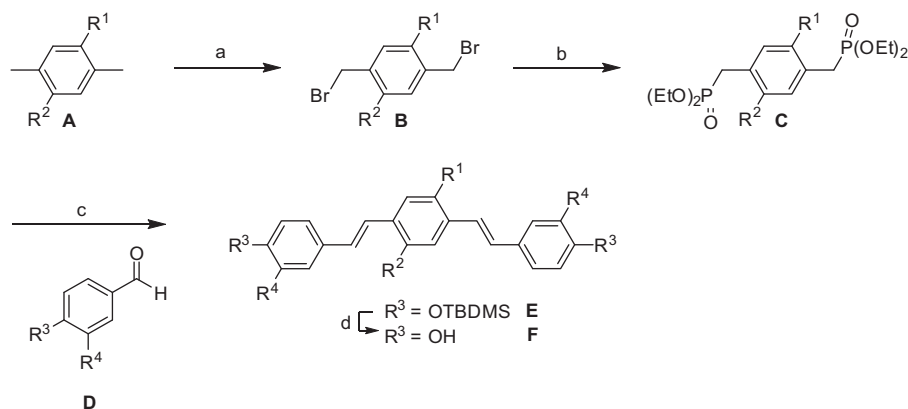
Figure 1. Previously reported amyloid- β binding ligands.

for the development as an MRI contrast agent. The initial breakthrough came with the design of compound **9** (FSB), which was specifically designed for in vivo detection of A β using ^{19}F MRI.¹¹ Since normal biological tissue completely lacks fluorine, ^{19}F MRI would allow direct imaging of the amyloid binding compound, without any endogenous background signal ('hot spot imaging'). Initial in vivo animal studies with compound **9** showed promising results. Unfortunately, ^{19}F MRI in vivo experiments suffer from the inherently low sensitivity of MRI with a detection limit in the micromolar to millimolar range depending merely on the voxel size and magnetic field strength. As initial ^{19}F compound only carried a single fluorine atom this makes ^{19}F MRI a technical challenge requiring long acquisition times. The incorporation of multiple magnetically equivalent ^{19}F atoms could aid with respect to this aspect, as the spin of each individual ^{19}F nucleus directly adds to the MR signal. The study therefore aimed to further exploit the bis-styrylbenzene backbone as a specific amyloid- β targeting MR contrast agent by increasing the number of fluorine atoms positioned to maintain favorable NMR characteristics as well as solubility. Synthesized compounds were evaluated with respect to their A β binding and specificity, and their fluorescent properties. Partition coefficients ($\log P$) were determined to assess hydrophobicity. Compounds were injected systemically in transgenic AD mice to determine BBB passage and affinity for amyloid plaques

in vivo. For the most promising compound, in vitro and post-mortem ^{19}F NMR studies were performed.

2. Design

Previously Flaherty et al. have designed a similar series of poly-fluorinated compounds, based on a bis-styrylbenzene structure with either a non-substituted core with fluorine substitutions on the outer rings, or four ^{19}F atoms on the inner ring with a polar substituent on the outer ring.¹² These compounds were found to target A β in vivo. As was already proven for Methoxy-X04 (**10**, Scheme 1), acidic functional groups are not required for high affinity A β binding, with the apparent K_d 's of these fluorinated compounds being ~ 300 fold lower compared to **9**. Despite their ability to label amyloid in vivo, however, the Flaherty compounds are very hydrophobic, and therefore their solubility and blood-brain barrier (BBB) passage are likely to limit their full potential as a ^{19}F MRI agent. Furthermore, positioning of the ^{19}F group directly on the planar backbone may have a detrimental effect on its relaxometry following binding, while it has been suggested that in addition to the inherent sensitivity of MRI also ^{19}F relaxivity plays an important role in the detection, due to a reduction of the transverse relaxation time (T_2) caused by binding to amyloid, or by a hydrophobic environment like brain tissue.¹³ Therefore,



	R ¹	R ²	R ³	R ⁴
10 (Methoxy-X04)	OMe	H	OH	H
11	OMe	OMe	OH	H
12	OMe	H	CH ₂ OH	H
13	OMe	H	CF ₃	H
14	OMe	H	OCF ₃	H
15	OMe	H	CF ₂ CF ₂ H	H
16	OH	H	CF ₃	H
17	OH	H	OCF ₃	H
18	OH	H	CF ₂ CF ₂ H	H
19	CF ₃	H	OH	H
20	OCH ₂ CF ₃	H	OH	H
21	O(CH ₂) ₃ CF ₃	H	OH	H
22	OC(CF ₃) ₃	H	OH	H
23	OH	H	OMe	CF ₃
24	OMe	H	OMe	CF ₃

Scheme 1. Reagents and conditions: (a) *N*-bromosuccinimide, benzoyl peroxide, CCl₄, reflux, 16 h; (b) triethyl phosphite, 150 °C, 16 h; (c) (1) KOtBu or NaH, THF, –10 or 0 °C, 20 min then **D**, rt, 16 h (d) tetra-*n*-butylammonium fluoride, THF, 0 °C, rt, 16 h.

we set out to extend the existing bis-styrylbenzene library by adding one or more polar moieties to improve solubility and increase the number of (magnetically equivalent) fluorine atoms positioned such to maintain favorable NMR characteristics.

As a starting point, Methoxy-X04 (**10**) was chosen.¹⁰ With an affinity for Aβ in the nanomolar range ($K_i = 26.8$ nM), this fluorescent small molecule is frequently used for intravital microscopy studies as it has high affinity for Aβ plaques in vivo following intravenous or intraperitoneal injection.¹⁴ We designed a series of bis-styrylbenzenes with incorporating multiple preferably magnetically equivalent fluorine atoms (**11–24**) or additional minor modifications (Scheme 1).

Compounds **11–24** are accessible from the general synthesis route given in Scheme 1, with the key building blocks being a diphosphonate (**C**) and an aromatic aldehyde (**D**). Substituted *p*-xylylene (**A**) is subjected to radical bromination to yield dibromide (**B**). This dibromide is then treated with triethyl phosphite in an Arbusov reaction to give diphosphonate (**C**). A Horner–Wadsworth–Emmons (HWE) reaction between diphosphonate (**C**) and an aldehyde (**D**) yields the (*E,E*)-bis-styrylbenzene (**E**). If necessary, an additional deprotection step with TBAF is carried out to remove the silyl protecting groups (only in the cases where the final compounds have hydroxyl substituents). Independently, a similar synthesis route for the design of NFT and amyloid probes based on styrylbenzenes was recently published by Boländer et al.¹⁵

The building blocks needed for the synthesis of compounds **10–24** are depicted in Figure 2, and were synthesized or commercially available. (For synthesis of all building blocks, see Supporting information.)

3. Fluorescent properties

All synthesized compounds are expected to have fluorescent properties based on their conjugated ring structures. We therefore determined excitation and emission wavelengths of 300 nM solutions and the corrected emission intensities were compared to that of Methoxy-X04 (Table 1).

It has been reported that binding to amyloid may have a significant effect on fluorescence properties,¹⁶ and therefore the fluorescence was also measured in the presence of synthetic Aβ fibrils. The parent compound **10** showed the highest intrinsic fluorescence with a 10-fold increase in the presence of amyloid fibrils. A similar increase was typically only observed for those compounds that only had minor modifications on the outer rings. Several previously reported Aβ-targeting fluorophores have shown a clear red-shifted emission spectrum following binding.^{17,18} Some of our compounds showed a similar red-shift; though resulting in multiple emission peaks in the spectrum (Fig. 3). This observation suggests the presence of multiple binding sites, similar to what has previously been reported, for example for Thioflavin.¹⁹

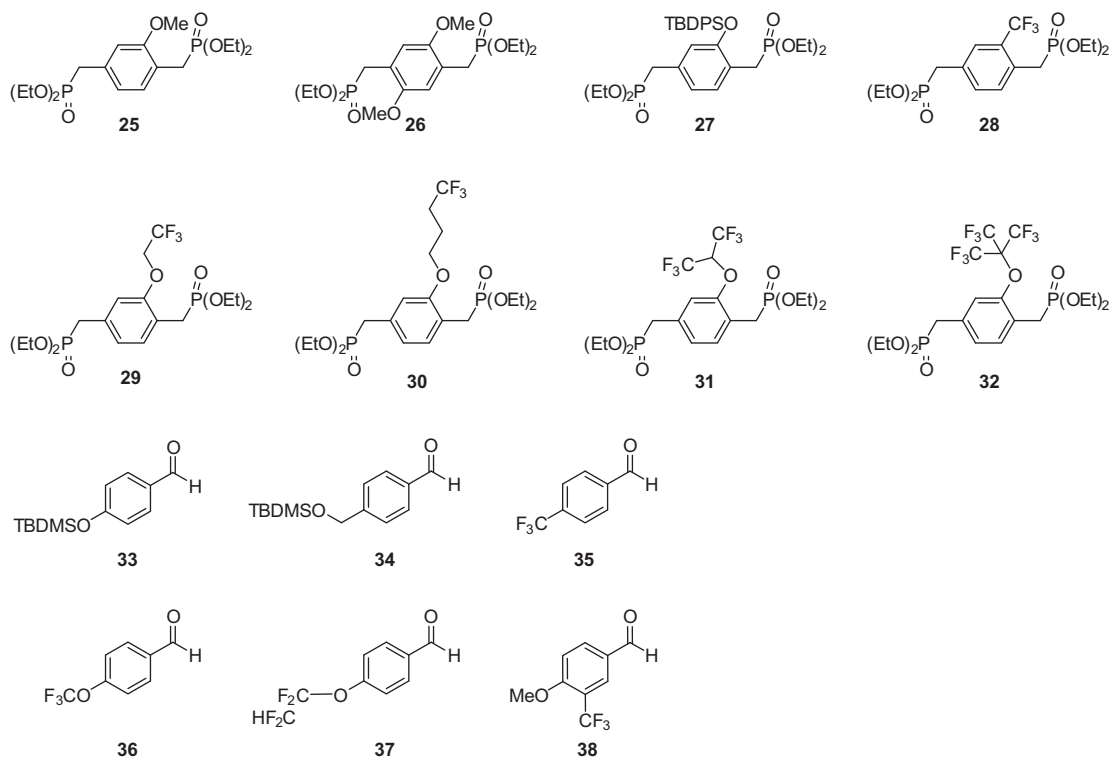


Figure 2. Structures of the building blocks 25–38.

4. Qualitative assessment of human and murine amyloid plaques binding

Fluorescence microscopy was used for a qualitative assessment of the amyloid-binding properties. A concentration series of each compound (1–10–100 μ M) was applied to brain slices of APP/PS1 mice and human AD patients. At 100 μ M all compounds, except **11** and **21**, showed characteristic staining of amyloid plaques on both human and murine sections. At the lower concentrations, however, clear differences in affinity were found (Table 1 & Fig. 4). Amyloid plaques in humans and mice differ in composition and compactness.²⁰ This is likely the reason that all compounds showed higher affinity for murine plaques as they were visible even after staining with 1 μ M concentration, whereas compounds **19–21** and **23–24** showed no detectable amyloid plaques in the human sections at this concentration. To illustrate these differences, Table 1 and Figure 4 highlight the results of the 10 μ M staining on human sections and the 1 μ M concentration used to stain the murine sections.

In general, planarity is considered one of the criteria for binding to A β plaques.²¹ The introduction of an additional substitution on the middle ring, which disturbs the planar conformation, has a detrimental effect on the binding affinity, as virtually no binding was seen using **11**.

Although previous studies have reported possible interaction of styrylbenzenes with NFTs,¹⁵ for none of our compounds NFTs staining was observed in the human AD cortex at these concentrations. Furthermore, with no background staining in either human or murine control brain sections this suggested their specificity to amyloid. As stated in the previous paragraph, the fluorescence intensity with and without amyloid fibrils differed significantly for the various compounds. Therefore, the fluorescence intensity in the presence of fibrils was calculated and expressed relative to the intensity of Methoxy-X04 (**10**) (Table 1). Assuming that the fluorescence yield in the presence of synthetic A β is representative

for that in the presence of amyloid plaques, the data in Figure 4 can be interpreted as follows. Despite having a lower fluorescent intensity for the bound compound, compounds **16–18** and **22** labeled more human amyloid, thus suggesting an improved binding compared to Methoxy-X04. Similar analysis of the stained APP/PS1 sections revealed the affinity of all compounds, except **11** and **21**, to be significantly higher than that of our lead compound Methoxy-X04 (K_d 26.8 nM). Compounds **13** and **15** were found to have the most efficient binding properties for murine amyloid plaques. With the lowest fluorescent intensity after binding to amyloid, being 100 \times less than Methoxy-X04, the murine amyloid plaques nonetheless appeared very bright.

5. Affinity for synthetic amyloid- β fibrils

A competition assay with [³H]chrysamine G (**6**) was used to determine the binding inhibition coefficient (K_i) for the compounds. Based on this assay reproducible results could only be obtained for those compounds with a hydroxyl substituent on the outer rings (Fig. 5). The ex vivo stainings clearly showed that many of the other compounds show affinity for amyloid, implying that these compounds probably use different binding sites than chrysamine G. Even the provided K_i values for compounds **19–23** only reflect competition against the [³H]chrysamine G binding sites, and therefore most likely underestimate the overall affinity of these compounds for synthetic A β fibrils.

6. LogP values

The blood–brain barrier (BBB) is a tight layer of endothelial cells in the wall of cerebral blood vessels that limits the passage of blood compounds into the brain. It is traditionally stated that for optimal passive BBB passage, compounds should preferably have moderately hydrophobicity (logD or logP 2.0–3.5) however a number of successful radiopharmaceuticals do not meet this requirement.²²

Table 1
Fluorescent and binding characteristics

Compound	MW (da)	Ex vivo A β binding ^a		λ_{ex}^b (all \pm 1 nm)	λ_{em} (all \pm 1 nm)	Fluorescence intensity ^c (%)	Fluorescence intensity on binding to fibrillar A β^d	Increase on binding to fibrillar A β	K_i (nM)
		Human	Murine						
10	344.403	+	+	372	451	100	100	9.8	24.2
11	374.429	–	–	n.d.	n.d.	n.p.	n.p.	n.p.	n.d.
12	372.456	+	++	360	436	63	26	4.1	n.d.
13	448.400	+	++	356	471	9	1	\sim 1	n.d.
14	480.399	+	++	354	456	31	3	\sim 1	n.d.
15	544.433	+	++	354	456	10	1	\sim 1	n.d.
16	434.374	++	++	351	464	6	2	3.6	n.d.
17	466.372	++	++	331	458	17	13	7.4	n.d.
18	530.407	++	++	325	487	7	n.d.	n.d.	n.d.
19	382.375	–	++	354	466	18	19	10.7	244
20	412.401	–	+	360	450	16	7	4.1	39.3
21	440.454	–	–	360	465	5	2	4.3	56.4
22	548.397	++	++	355	472	21	38	17.8	84.48
23	494.426	–	++	355	472	17	2	\sim 1	n.d.
24	508.452	–	++	355	494	37	4	\sim 1	n.d.

n.d. = not detected; n.p. = not performed.

^a Staining of amyloid plaques in human (10 μ M) and APP-PS1 murine (1 μ M) was scored whether the compound stained less (–), similar (+) or more (++) for amyloid plaques in comparison to **10**.

^b Ex/Em wavelength maxima were determined of 300 nM solutions.

^c Fluorescence intensity was calculated relative to **10**.

^d Fluorescence intensity was calculated relative to intensity of **10** after binding to fibrillar A β .

Therefore $\log P$ or $\log D$ should be considered carefully as selection criterion, but it is a valid parameter for selection nonetheless when applied within one series of compounds. For each of our compounds **10–24**, $\log P$ values were determined with an HPLC-based method according to Benhaim and Grushka.^{23–25} The found $\log P$ values are shown in Table 2. The limitation of this method is that $\log P$ values > 7 cannot be measured reliably. Not surprisingly, many of the compounds actually do show $\log P$ values > 7 , which is a logical consequence of the fact that Methoxy-X04 (**10**) itself already has a $\log P$ value of 5.05 and that the introduction of fluorine makes the molecules more hydrophobic.

7. In vivo amyloid plaque labeling in transgenic AD mice

To assess the ability of the compounds to pass the BBB in vivo and subsequently bind to amyloid, solutions of each compound were injected intravenously in living transgenic APP/PS1 mice that had

extensive cerebral amyloid plaques. The mice were sacrificed, their brains were removed and post-mortem sections were studied using the same fluorescence microscopy set-up as for the stained brain sections. In vivo labeling of amyloid plaque was observed for almost all compounds, except **11**, **23** and **24**, showing their ability to pass the BBB. (Fig. 4 and Table 2) Apparently, a high $\log P$ value does not necessarily prohibit BBB passage. Some compounds, particularly **13**, showed a comparable signal intensity after intravenous injection compared to Methoxy-X04, despite having a 100-fold lower fluorescence yield. This suggests that these compounds have a high affinity and/or cross the BBB more efficiently than Methoxy-X04.

8. In vitro and post-mortem fluorine NMR

Based on the above experiments, compounds **13** and **22** were identified as the most promising leads, based on favorable binding, and positive staining after intravenous injection in vivo indicating

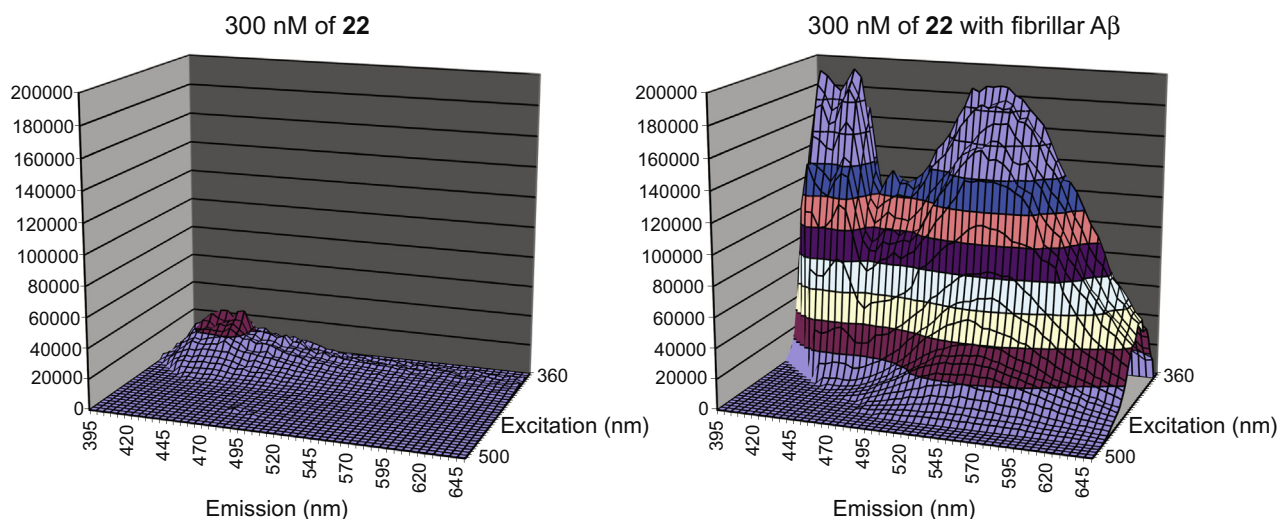


Figure 3. Excitation and emission spectra of compound **22**. Shown are the excitation/emission spectra of compound **22** to illustrate possible effects on the fluorescent properties following binding of amyloid.

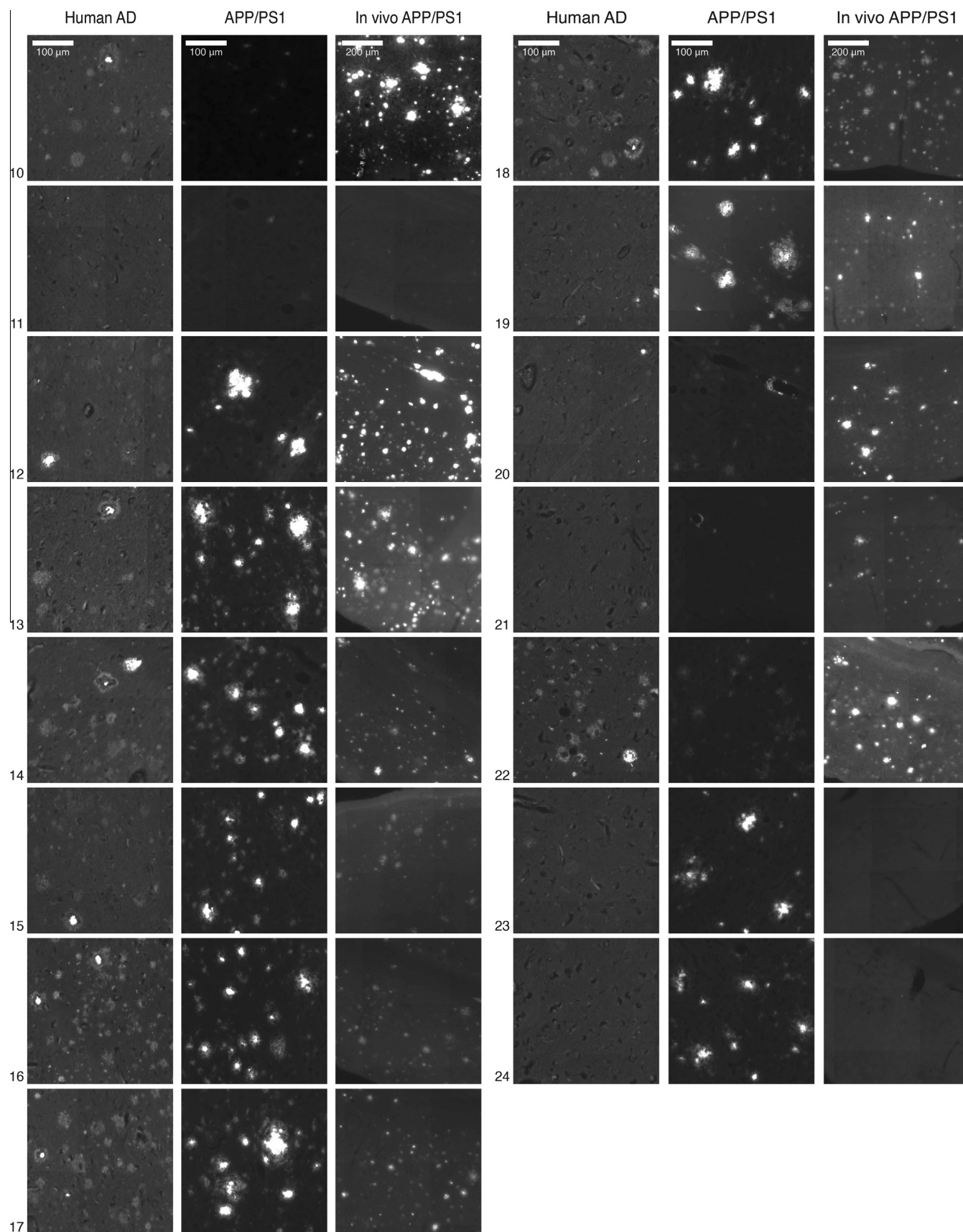


Figure 4. Staining for murine and human amyloid plaques. Shown paraffin embedded 8 μm thick human AD sections are stained using 10 μM, whereas APP/PS1 murine sections are stained using 1 μM to best depict the differences in amyloid staining between the different compounds. Thirty micrometer thick murine APP/PS1 sections following in vivo administration are shown with two times less magnification to allow visualization of a larger cortical region. All images were digitized using the same settings.

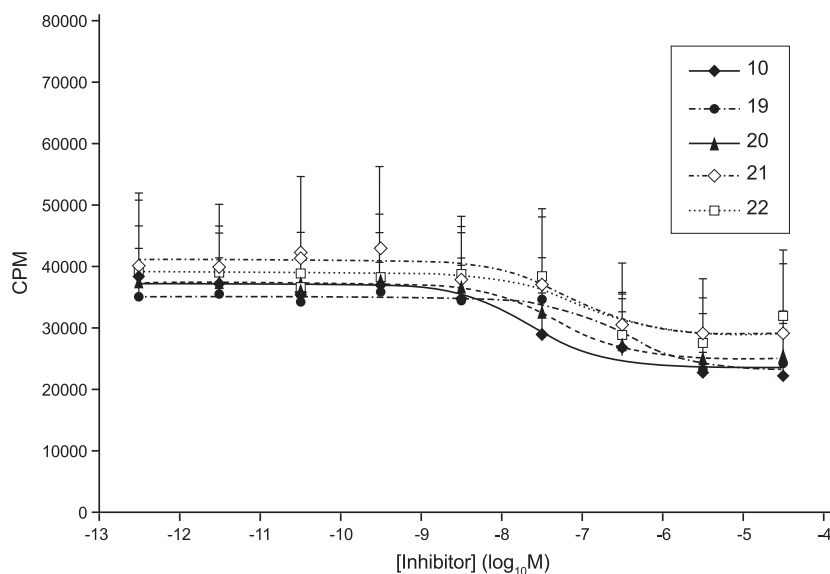


Figure 5. Non-linear fitting to assess affinity for synthetic amyloid- β fibrils by a competition assay with [^3H]chrysaline G.

Table 2
Log P values and scoring of amyloid labeling following intravenous injection

Compound	Log P (calcd) ^a	Log P (determined)	In vivo amyloid labeling
10	5.55	4.84	+
11	5.46	5.00	–
12	5.53	4.99	+
13	9.06	>7	+
14	8.44	>7	+
15	10.04	>7	+
16	8.74	6.18	+
17	8.12	>7	+
18	9.72	>7	+
19	6.74	5.64	+
20	6.83	5.25	+
21	7.37	5.79	+
22	10.22	>7	+
23	8.57	7.17	–
24	8.89	>7	–

The ability to label amyloid plaques in the brains of APP-PS1 mice following intravenous injection were scored absent (–) or present (+).

^a Log P values were calculated used web-based methods: www.molinspiration.com and <http://intro.bio.umb.edu/111-112/OLLM/111F98/jlogp/test.html>.

good BBB passage. Initial ^{19}F NMR studies were only conducted with compound **22**, which had the highest number of magnetically equivalent ^{19}F atoms. NMR spectra were acquired for 1.92 mM of **22** with or without an excessive amount of fibrillar A β . Binding to fibrillar amyloid did not result in significant line broadening of the NMR spectrum. (Fig. 6A) The NMR spectrum corresponding to compound **22** mixed with homogenized APP/PS1 brain, however, revealed a small chemical shift of 0.03 ppm and a severe reduction in T_2 as observed by the line broadening of the peak. As suggested previously, most likely the lipophilic environment of the brain tissue itself results in a reduced relaxation time and thereby signal loss.¹³

Finally, 30 $\mu\text{mol}/\text{kg}$ of **22** was injected intravenously in APP/PS1 mice. The brains were removed after 24 h and a ^{19}F NMR spectrum was obtained of the brain homogenate. No ^{19}F signal was observed, although antemortem intravital microscopy showed clear labeling of cerebral amyloid (Fig. 6B–C).

The severe attenuation of the ^{19}F NMR signal due the hydrophobic nature of both the fluorinated compounds as well as the brain itself seemed to hampered the detection of the ^{19}F signal in the

mouse brain. This is contrary to the initial publication of a ^{19}F amyloid ligand by Higuchi et al.,¹¹ but in agreement with the findings of Amatsubo et al.¹³ Our design balanced between the planarity needed for amyloid binding and free rotation for the fluorine groups to maintain favourable NMR characteristics, however, this data still suggests that the hydrophobic interaction between the brain and the ^{19}F groups are responsible for line broadening. As recently pointed out in vivo by Yanagisawa et al. this problem might be overcome by the use of a polyethylene glycol (PEG) linker to attach the fluorine groups further away from the amyloid binding core.²⁶

9. Summary and conclusion

In this work, a series of 15 analogs of Methoxy-X04 (**10**) with various number of fluorine atoms has been synthesized and evaluated for their A β binding properties and ability to pass the BBB. The incorporation of suitably placed fluoro substitutions could improve the current (MRI) contrast agents for the diagnosis of Alzheimer's disease. It was concluded that the introduction of a second substitution on the inner ring was not well tolerated, whereas single bulky modifications on both the outer and inner rings were well tolerated. Despite the observed high log P values brain entry did not seem to be inhibited for most compounds. Based on all findings, compounds **13** and **22** were considered most promising for the development of A β imaging agents. However, the post-mortem NMR results leave us to conclude that there seems to be no role for these compounds as MR imaging agents for the diagnosis of AD. To our opinion it remains doubtful whether the incorporation of other fluorine moieties or higher field magnetic field strength will help to overcome these hurdles next to those set by the inherent relatively low sensitivity of ^{19}F MRI in combination with known cerebral A β concentrations.

Nevertheless, this study expands the existing knowledge on bis-styrylbenzenes as amyloid targeting agents in general and creates opportunities for their application as fluorescent amyloid ligands for preclinical optical imaging. Recent advances in fluorine chemistry create further opportunities to radiolabel compounds of our series with ^{18}F .^{27,28} These compounds might provide additional information regarding accumulation of cerebral amyloid, especially since we have found that our series of compounds bind to a distinct binding site.

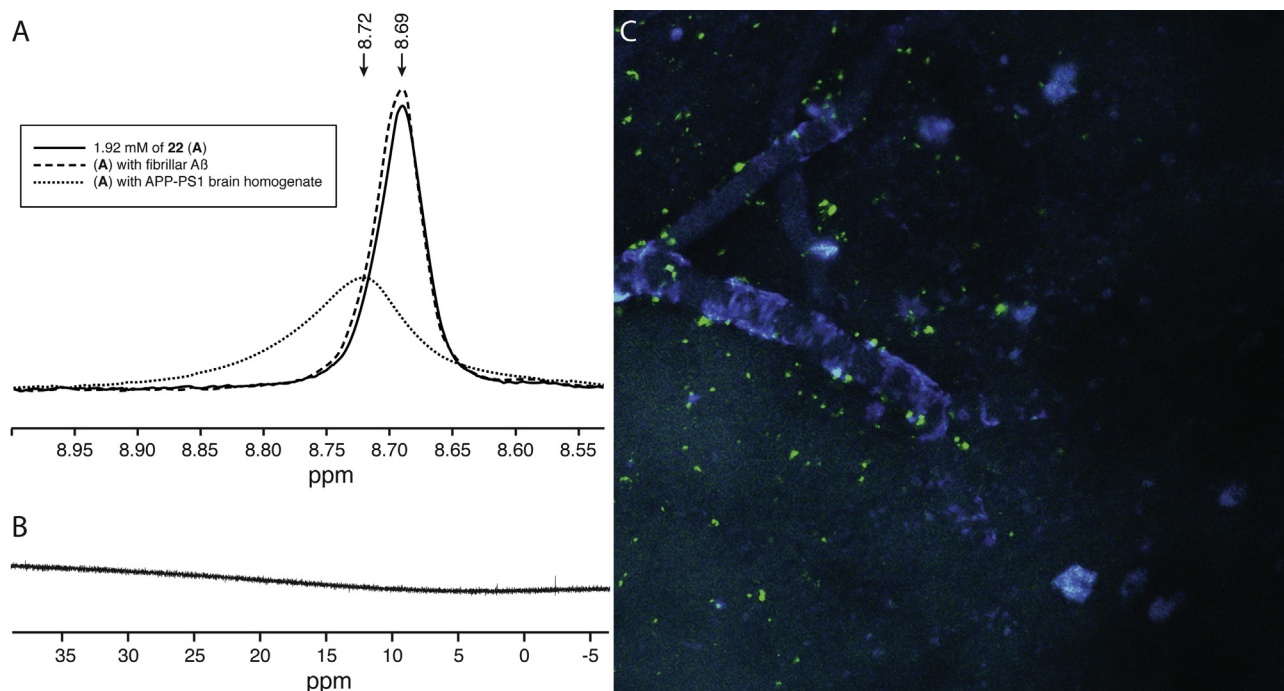


Figure 6. In vitro and post-mortem ^{19}F NMR analyses of compound **22**. (A) Shows the NMR spectra corresponding to 1.92 mM of compound **22** in solution without (-) or with the presence of 22 μM fibrillar $\text{A}\beta$ (- -) or mixed with a homogenized aged APP/PS1 mouse brain. All spectra are relative to trifluoroacetic acid set at 0 ppm. (B) shows a NMR spectra of a homogenized APP/PS1 mouse brain made 24 h post-injection of 30 $\mu\text{mol}/\text{kg}$ of dissolved **22**. The corresponding intravital microscopic image presented in (C) clearly shows the antemortem labeling of cerebral amyloid (blue) in both vasculature as well as parenchymal amyloid plaques. Image dimensions are 615 \times 615 μm .

10. Experimental section

10.1. Preparation of $\text{A}\beta_{1-40}$ fibrils

$\text{A}\beta$ fibrils were prepared by stirring a 0.5 mg/ml solution of $\text{A}\beta$ peptide (1–40) (RPeptide, Bogart, GA) at 37 $^{\circ}\text{C}$ for 3 days, which resulted in a cloudy solution. The presence of fibrils was confirmed by the appearance of an emission peak at 482 nm (excitation 440 nm) upon addition of a 5 μM solution in PBS of Thioflavin T (Sigma, Germany) to a small amount of fibrils. Aliquots of 10 μl were transferred to Eppendorf vials and stored at -80°C until the assay was to be performed.

10.2. Fluorescence spectra

All compounds were dissolved in DMSO at 0.3 mM and diluted to 300 nM with 9:1 PBS/ethanol. Fluorescence spectra were measured on a Varian Cary Eclipse fluorescence spectrophotometer to obtain peak excitation and emission wavelengths, which were used to select the correct fluorescence filter settings for further microscopic evaluation. All measurements were carried out at 20 $^{\circ}\text{C}$ and in triplicate. 3D fluorescence spectra were obtained by adding 500 μl of the dissolved compounds to previously prepared $\text{A}\beta$ aliquots. After manual shaking for 30 s, 300 μl samples were measured (Infinity M1000, Tecan, Switzerland).

10.3. Staining of human and transgenic AD brain sections

Stock solutions of 3 mM in DMSO were diluted to 1–10–100 μM in 2:3 PBS/ethanol and sonicated for 15 min. Paraffin sections (8 μm) of the medial temporal lobe cortex of human AD subject that was assigned as Braak IV, 14 months old transgenic murine APP/PS1 brain and age-matched control cortices were deparaffinized prior to staining for 10 min in absolute darkness. After gently rinsing with tap water, sections were placed in 0.1% NaOH in 80%

ethanol for 2 min, air dried and coverslipped using Aqua/Poly-mount. Fluorescence of the stained sections was analyzed using a whole microscopic slide scanner (Pannoramic MIDI, 3DHitech, Hungary) with a DAPI filter cube (Ex 365 nm; Em 445/50 nm) using the same intensity setting throughout all experiments.

10.4. In vivo $\text{A}\beta$ plaque labeling in transgenic AD mice

Twelve-to-fourteen-month-old APP/PS1 mice or age-matched wildtype animals ($n = 2$ per compound) were injected intravenously with 0.05 M dissolved in 1:1 DMSO/Cremophor diluted with PBS to a total volume of 200 μl , resulting in a total dose of 30 $\mu\text{mol}/\text{kg}$. One day after injection, animals were sacrificed using 200 μl Euthanasol (AST Pharma) prior to transcardial perfusion with 4% paraformaldehyde in PBS. Brains were removed and cryoprotected in 4% PFA with 10% sucrose for 4 hours followed by immersion in 4% PFA with 30% sucrose overnight. Snap-frozen brains were cryosectioned (30 μm) and fluorescence images were analyzed as described above.

10.5. Competition binding assay

Competition binding experiments were conducted at room temperature, in a final volume of 1 ml assay buffer (150 mM Tris-HCl, 20% ethanol, pH 7.0). Compounds were dissolved as 3 mM stock solutions in DMSO, sonicated for 15 min, and used in a final concentration range of 30 μM to 30 pM. 10 μl of unlabeled test compounds was combined with 890 μl of assay buffer and 50 μl of 100 nM [^3H]-chrysamine G stock (specific activity 33.8 Ci/mmol). The mixture was sonicated for 10 min, and the assay was subsequently started by the addition of 50 μl synthetic $\text{A}\beta_{1-40}$ fibrils, to achieve final concentrations of 5 nM [^3H]-chrysamine G and 50 nM fibrils. Nonspecific binding was determined in the presence of 1 μM Methoxy-X04. Incubations were terminated after 1 h via filtration through Whatman GF/B filters

(pre-soaked in binding buffer), using a 48-well Brandel harvester. The filters were washed two times with 3 ml of ice-cold binding buffer (pH 7.0), and radioactivity was determined by liquid scintillation spectrometry in 5 ml of Optiphase-HiSafe 3, at an efficiency of 40%.

K_i values were determined by nonlinear regression analysis using the equation: $\log EC_{50} = \log[10^{\log K_i} * (1 + \text{radioligand}/K_d)]$ where $K_d = 200$ nM, and radioligand = 5 nM. (GraphPad Software Inc., San Diego, CA).

10.6. Procedure for logP determinations

LogP determinations were performed using literature procedures.²³ The measurements were performed on a Jasco HPLC-system (detection simultaneously at 214 and 254 nm) coupled to a Perkin Elmer Sciex API 165 mass instrument with a custom-made Electrospray Interface (ESI). An analytical Gemini C₁₈ column (Phenomenex, 50 × 4.60 mm, 3 micron) was used in combination with buffers A: phosphate buffer of pH = 7.0 (0.02 M Na₂HPO₄ adjusted to pH = 7.0 with phosphoric acid) and B: 0.25% octanol in methanol.

Of all compounds to be evaluated, stock solutions of 0.5 mg ml⁻¹ were prepared in methanol. These stock solutions were then diluted with water, making sure that the volume percentage of water was such that the compounds did not precipitate (max 40% water). A 0.25 mg ml⁻¹ solution of NaNO₃ in water was used as a non-retaining compound to determine the dead time of the system. For calibration purposes known compounds were taken from the literature. Of these compounds, 0.25 mg ml⁻¹ solutions in either 75% H₂O/MeOH or 50% H₂O/MeOH were made.

For each sample, a series of four isocratic runs was performed, (for instance 55%, 60%, 65%, 70% B), and the retention times (from UV-detection at 214 nm) thus obtained were converted to the retention factor k' according to the formula $k' = (t_R - t_0)/t_0$, with t_R being the retention time of the compound and t_0 being the retention time of NaNO₃. The retention factors were extrapolated to 0% B, yielding k'_w . As there is a linear relationship between logP and log k'_w plotting logP values of known compounds (Table 3) against obtained log k'_w values in this system yields a calibration curve. From this curve, logP values of unknown compounds can be calculated from their k'_w values.

10.7. In vitro ¹⁹F NMR analyses

To investigate the possible effect on its NMR properties caused by either binding to amyloid or the lipophilic environment of the brain several samples were prepared similar to the protocol described previously.¹³ The in vitro ¹⁹F NMR analyses were performed using a Bruker DMX400 NMR spectrometer (Bruker, Germany). All samples were diluted with 10% D₂O in 0.1 M PBS with one EDTA-free protease inhibitor tablet (Complete Mini,

Roche Diagnostics) added to every 10 ml. Aliquots (500 μl) of only the solvent, the solvent containing 22 μM of aggregated Aβ or the brain homogenate were added to 20 μl of 0.05 M of **22** in 1:1 DMSO/Cremophor to achieve a final concentration of 1.92 mM of compound **22**. The mixtures were transferred to a standard 5 mm NMR tube. NMR spectra were obtained using a single pulse sequence with a 22,573 Hz spectral width (SW) and 100 scans. The chemical shifts of the ¹⁹F NMR signals were identified by setting the reference trifluoroacetic acid (TFA) at 0 ppm.

10.8. Post-mortem ¹⁹F NMR in APP/PS1 mice

Twelve-to-fourteen-month-old APP/PS1 mice ($n = 2$) received an intravenous injection with 0.05 M of compound **22** dissolved in 1:1 DMSO/Cremophor diluted with PBS to a total volume of 200 μl to achieve a total dose of 30 μmol/kg. Prior injection the animals underwent cranial window surgery.¹⁴ Twenty four hours post injection the animals underwent in vivo multiphoton microscopy (LSM 710 MP, Carl Zeiss, Germany) operating at 750 nm to validate the presence and labeling of cerebral amyloid. After perfusion the resected brain was snap frozen and prepared for NMR similar to the above brain homogenates. A similar fluorine NMR spectrum was obtained using a single pulse sequence with a 94,340 Hz SW and 1200 scans.

10.9. Synthetic procedures

10.9.1. General

Reagents and solvents were used as provided, unless stated otherwise. 4-Trifluoromethylbenzaldehyde (**35**), 4-trifluoromethoxybenzaldehyde (**36**), 4-(1,1,2,2-tetrafluoroethyl)benzaldehyde (**37**), 3-trifluoromethyl-4-methoxybenzaldehyde (**38**) (Fig. 2) were purchased at standard suppliers. The other building blocks as shown in Figure 2 were prepared following literature procedures (see supporting info). THF was distilled over LiAlH₄ prior to use. Reactions were carried out under inert conditions and ambient temperature, unless stated otherwise. Prior to performing a reaction, traces of water were removed from the starting materials by repeated coevaporation with anhydrous 1,4-dioxane or anhydrous toluene. These solvents were stored over 4 Å molsieves. Reactions were monitored by thin layer chromatography on aluminum coated silica sheets (Merck, silica 60 F254), using visualization either with iodine, or spraying with a solution of 25 g (NH₄)₂MoO₄, 10 g (NH₄)₄Ce(SO₄)₄ in 100 ml H₂SO₄ and 900 ml H₂O, or a solution of 20% H₂SO₄ in ethanol, followed by charring at ~150 °C. Column chromatography was carried out with silica gel (Screening Devices bv, 40–63 μm particle size, 60 Å), using technical grade solvents. NMR spectra were recorded at 298 K on a Bruker AV400 using deuterated solvents. All carbon spectra are proton-decoupled. Chemical shifts (δ) are given in ppm, in ¹³C spectra relative to the solvent peaks of CDCl₃ (77.0 ppm), CD₃OD (49.0 ppm), DMF-*d*₇ (29.76 ppm), acetone-*d*₆ (29.9 ppm) or DMSO-*d*₆ (39.51 ppm), in ¹H spectra relative to the solvent peak of tetramethylsilane (0.0 ppm), CD₃OD (3.31 ppm), DMF-*d*₇ (2.75 ppm), acetone-*d*₆ (2.05 ppm) or DMSO-*d*₆ (2.50 ppm), in ¹⁹F spectra relative to the solvent peak of TFA (0 ppm). Coupling constants are given in Hz. IR spectra were recorded on a Perkin Elmer Paragon 1000 FT-IR Spectrometer. High resolution mass spectra were recorded by direct injection (2 μl of a 2 μM solution in H₂O/MeCN; 50:50; v/v and 0.1% formic acid) on a mass spectrometer (Thermo Finnigan LTQ Orbitrap) equipped with an electrospray ion source in positive mode (source voltage 3.5 kV, sheath gas flow 10, capillary temperature 250 °C) with resolution $R = 60,000$ at m/z 400 (mass range $m/z = 150$ –2000) and dioctylphthalate ($m/z = 391.28428$) as a “lock mass”. The high resolution mass spectrometer was calibrated prior to measurements with a calibration mixture (Thermo Finnigan). It should be noted

Table 3
Reference logP values

Compound	LogP
Resorcinol	0.8
<i>p</i> -Nitroaniline	1.39
phenol	1.46
<i>m</i> -Nitrophenol	2
2-Naphtol	2.7
Naphtalene	3.37

Based on known literature values, the logP of several reference compounds yield a required calibration curve to determine the logP values of our compounds.^{21–23}

that, with the exception of compound **9** (data not shown) and only certain intermediates ionized correctly, none of the target compounds provided useful (HR)MS data.

LC–MS analysis was performed on a Finnigan Surveyor HPLC system with a Gemini C₁₈ 50 × 4.6 mm column (3 micron, Phenomenex, Torrance, CA, USA) (detection at 200–600 nm), coupled to a Thermo Finnigan LCQ Advantage Max mass spectrometer (Breda, The Netherlands) with electrospray ionization (ESI; system 1), with as eluents (A): H₂O; (B): MeCN and (C): 1% aq TFA.

10.9.1.1. General procedure A: Horner–Wadsworth–Emmons reaction with NaH. The diphosphonate (0.83 mmol) was dissolved in THF (2.6 mL) and cooled to 0 °C. NaH (60% wt. dispersion in mineral oil, 0.17 g, 4.17 mmol) was added and the mixture stirred for 30 min at 0 °C. The aldehyde (2.08 mmol) was dissolved in THF and added to the reaction mixture, which was subsequently stirred for 16 h at rt. After cooling and quenching with water, the mixture was extracted three times with EtOAc and the combined organic layers were washed with satd aq NaHCO₃, dried (Na₂SO₄), filtered and concentrated. The crude product was subjected to column chromatography to yield the pure product.

10.9.1.2. General procedure B: Horner–Wadsworth–Emmons reaction with KOtBu. The diphosphonate (0.95 mmol) was dissolved in THF (20 mL) and cooled to –10 °C. KOtBu (0.30 g, 2.45 mmol) was added and the black mixture stirred for 20 min. A solution of the aldehyde (2.37 mmol) in THF (6 mL) was added and the reaction stirred at rt for 16 h. The reaction was cooled to 0 °C, quenched with water and extracted five times with EtOAc. The combined organic layers were dried (Na₂SO₄), filtered and concentrated. The crude product was subjected to column chromatography to yield the pure product.

10.9.1.3. General procedure C: silyl deprotection. A solution of protected bis-styrylbenzene (0.63 mmol) in THF (2 mL) was cooled to 0 °C and TBAF (1 M in THF, 3.14 mL, 3.14 mmol) was added. The blood-red solution was stirred for 16 h after which water was added and the reaction mixture was extracted with EtOAc. To the aqueous layer 1 N HCl was added, followed by two times extracting with EtOAc. The combined organic layers were dried (Na₂SO₄), filtered and concentrated. The pure product was obtained by column chromatography (0 → 25% EtOAc/light petroleum).

10.9.1.4. (E,E)-1-Methoxy-2,5-bis(4-hydroxy)styrylbenzene; Methoxy-X04 (10). Methoxy-X04 was prepared according to general procedures **A** and **C**, using diphosphonate **25** and aldehyde **33**. Physical data corresponded to those reported in Ref. ¹⁰.

10.9.1.5. (E,E)-1,4-Dimethoxy-2,5-bis(4-hydroxy)styrylbenzene (11). Following general procedure **A**, diphosphonate **26** (0.34 g, 0.78 mmol) was reacted with aldehyde **33** (0.46 g, 1.9 mmol). A bright yellow solid was isolated (221 mg) by column chromatography (10 → 30% EtOAc/light petroleum) of which 100 mg was purified by preparative HPLC (40:60 → 20:80 of 20 mM NH₄OAc/MeOH), to yield 22 mg (0.059 mmol, 8%) of compound **11**.

¹H NMR (CD₃OD, 400 MHz): δ 7.43 (d, *J* = 8.6 Hz, 4H); 7.33 (d, *J* = 16.5 Hz, 2H); 7.27 (s, 2H); 7.19 (d, *J* = 16.5 Hz, 2H); 6.82 (d, *J* = 8.6 Hz, 4H); 3.93 (s, 6H). ¹³C NMR (CD₃OD, 100 MHz): δ 158.5; 152.6; 130.9; 129.7; 128.9; 127.6; 121.1; 116.6; 109.9; 56.8. IR (neat): 3359.6; 1605.3; 1515.7; 1495.6; 1463.6; 1435.4; 1408.7; 1260.0; 1196.0; 1171.8; 1022.4; 958.3; 849.6; 819.7; 790.1; 685.9; 551.0; 521.6. LC–MS retention time: 8.99 min (10 → 90% MeCN, 15 min run).

10.9.1.6. (E,E)-1-Methoxy-2,5-bis(4-hydroxymethyl)styrylbenzene (12). Following general procedure **A**, diphosphonate **25** (0.2 g, 0.5 mmol) was reacted with aldehyde **34** (0.31 g,

1.25 mmol). The crude product was subjected to column chromatography (0 → 2% EtOAc/light petroleum) to yield the intermediary bis-TBDMS protected styrylbenzene (0.28 g, 0.48 mmol, 96%) as a bright yellow solid. ¹H NMR (CDCl₃, 400 MHz): δ 7.58 (d, *J* = 8.1 Hz, 1H); 7.51 (d, *J* = 6.1 Hz, 2H); 7.49 (d, *J* = 6.3 Hz, 2H); 7.44 (s, 1H); 7.34–7.28 (m, 4H); 7.16–7.13 (m, 2H); 7.13–7.09 (m, 2H); 7.03 (d, *J* = 1.4 Hz, 1H); 4.75 (d, *J* = 2.4 Hz, 4H); 3.95 (s, 3H); 0.95 (s, 9H); 0.95 (s, 9H); 0.11 (s, 6H); 0.11 (s, 6H). ¹³C NMR (CDCl₃, 100 MHz): δ 157.0; 141.0; 140.7; 137.9; 136.7; 136.0; 128.7; 128.4; 128.1; 126.4; 126.4; 126.4; 126.0; 122.7; 119.3; 108.6; 64.9; 64.8; 55.6; 26.0; 18.4; –5.2. IR (neat): 2953.7; 2927.5; 2855.3; 1593.8; 1553.7; 1515.3; 1458.3; 1421.9; 1377.6; 1248.7; 1206.0; 1084.2; 1037.1; 1005.7; 967.3; 837.4; 773.9; 668.1; 504.2. The bis-TBDMS protected (*E,E*)-styrylbenzene (0.27 g, 0.46 mmol) was treated with TBAF according to general procedure **C**. Compound **12** was obtained by column chromatography (50% EtOAc/light petroleum → 10% MeOH/EtOAc) as a bright yellow solid (0.14 g, 0.37 mmol, 79%).

¹H NMR (DMF-*d*₇, 400 MHz): δ 7.68 (d, *J* = 8.0 Hz, 1H); 7.59 (d, *J* = 8.1 Hz, 2H); 7.55 (d, *J* = 8.1 Hz, 2H); 7.49 (d, *J* = 16.6 Hz, 1H); 7.39–7.34 (m, 4H); 7.31 (d, *J* = 5.0 Hz, 2H); 7.28 (d, *J* = 4.9 Hz, 1H); 7.25–7.21 (m, 2H). ¹³C NMR (DMF-*d*₇, 100 MHz): δ 157.7; 142.6; 142.3; 138.8; 137.2; 136.6; 129.0; 128.9; 128.4; 127.4; 126.8; 126.8; 126.6; 126.0; 122.9; 119.7; 109.3; 63.8; 55.6. IR (neat): 1592.0; 1557.6; 1515.8; 1455.9; 1418.0; 1340.0; 1269.9; 1243.7; 1211.9; 1158.1; 1112.4; 1034.2; 1011.7; 956.3; 825.7; 624.2.

10.9.1.7. (E,E)-1-Methoxy-2,5-bis(4-trifluoromethyl)styrylbenzene (13). Following general procedure **A**, diphosphonate **26** (0.20 g, 0.5 mmol) was reacted with aldehyde **35** (0.22 g, 1.25 mmol). After work-up, the crude product was purified by column chromatography (0 → 1% EtOAc/light petroleum) and the compound **13** was obtained as a bright yellow solid (80 mg, 0.18 mmol, 36%).

¹H NMR (acetone-*d*₆, 400 MHz): δ 7.82 (d, *J* = 8.2 Hz, 2H); 7.79 (d, *J* = 8.5 Hz, 2H); 7.76–7.69 (m, 5H); 7.66 (d, *J* = 16.7 Hz, 2H); 7.43 (s, 2H); 7.38 (d, *J* = 16.4 Hz, 2H); 7.29 (dd, *J* = 8.1 Hz, *J* = 1.3 Hz, 1H); 4.00 (s, 3H). ¹³C NMR (acetone-*d*₆, 100 MHz): δ 158.5; 143.0; 142.4; 139.3; 132.1; 128.3; 128.3; 127.9; 127.9; 127.8; 126.7; 126.5; 126.5; 126.5; 120.7; 110.3; 56.1. ¹⁹F NMR (acetone-*d*₆, 375 MHz): δ 12.70 (s, 3F); 12.65 (s, 3F). IR (neat): 1608.4; 1464.0; 1420.1; 1323.6; 1246.5; 1158.5; 1116.6; 1105.9; 1065.5; 1036.4; 1014.1; 967.0; 954.2; 866.5; 848.8; 829.9; 759.2; 744.8; 622.2; 593.3; 508.4.

10.9.1.8. (E,E)-1-Methoxy-2,5-bis(4-trifluoromethoxy)styrylbenzene (14). Following general procedure **A**, diphosphonate **25** (0.20 g, 0.5 mmol) was reacted with aldehyde **36** (0.24 g, 1.25 mmol). After work-up, the product **14** was obtained by column chromatography (0 → 1.5% EtOAc/light petroleum) as a bright yellow solid (83 mg, 0.17 mmol, 35%).

¹H NMR (CDCl₃, 400 MHz): δ 7.56 (d, *J* = 8.0 Hz, 1H); 7.54–7.50 (m, 4H); 7.44 (d, *J* = 16.5 Hz, 1H); 7.19 (t, *J* = 7.8 Hz, 4H); 7.14–7.10 (m, 2H); 7.09–7.05 (m, 2H); 7.01 (d, *J* = 1.3 Hz, 1H); 3.94 (s, 3H). ¹³C NMR (CDCl₃, 100 MHz): δ 157.2; 137.7; 136.7; 135.9; 127.7; 127.5; 127.2; 126.6; 125.9; 124.1; 121.2; 121.1; 119.4; 108.5; 55.5. ¹⁹F NMR (CDCl₃, 375 MHz): δ 19.80 (s, 3F); 19.79 (s, 3F). IR (neat): 1593.1; 1557.6; 1510.2; 1421.9; 1254.6; 1199.8; 1159.4; 1104.9; 1034.0; 1015.7; 962.2; 921.6; 838.6; 673.8; 620.1; 530.0; 505.9.

10.9.1.9. (E,E)-1-Methoxy-2,5-bis(4-{1,1,2,2-tetrafluoroethyl})styrylbenzene (15). Following general procedure **A**, diphosphonate **25** (0.20 g, 0.5 mmol) was reacted with aldehyde **37** (0.28 g,

1.25 mmol). After work-up, compound **15** was isolated by column chromatography (0 → 7.5% EtOAc/light petroleum) as a yellow solid (0.14 g, 0.25 mmol, 50%).

¹H NMR (CDCl₃, 400 MHz): δ 7.56 (d, *J* = 7.3 Hz, 1H); 7.55–7.49 (m, 4H); 7.33 (d, *J* = 16.5 Hz, 1H); 7.24–7.16 (m, 4H); 7.13–7.04 (m, 4H); 7.01 (d, *J* = 2.3 Hz, 1H); 6.07–5.76 (m, 2H); 3.94 (s, 3H). ¹³C NMR (CDCl₃, 100 MHz): δ 157.1; 148.5; 148.2; 137.7; 136.4; 135.6; 129.2; 128.7; 127.9; 127.8; 127.6; 127.5; 127.2; 126.6; 125.8; 122.4; 121.9; 121.8; 121.8; 121.7; 119.4; 119.1; 116.7; 116.4; 116.2; 115.5; 110.2; 108.7; 108.1; 107.7; 107.3; 55.5. ¹⁹F NMR (CDCl₃, 375 MHz): δ -10.5 (s, 4F); -59.06 (t, *J* = 5.5 Hz, 2F); -59.20 (t, *J* = 5.5 Hz, 2F). IR (neat): 1510.5; 1463.9; 1421.9; 1392.9; 1302.4; 1274.0; 1195.2; 1115.4; 1035.7; 1015.7; 961.8; 837.0; 784.1; 766.2; 709.4; 623.3; 600.0; 544.1.

10.9.1.10. (E,E)-1-Hydroxy-2,5-bis(4-trifluoromethyl)styrylbenzene (16). Following general procedure **B**, diphosphonate **27** (0.85 g, 1.34 mmol) was reacted with aldehyde **35** (0.59 g, 3.36 mmol). After work-up, the crude product was purified by column chromatography (0 → 6% EtOAc/light petroleum) and product **16** was obtained as a bright yellow solid (0.2 g, 0.48 mmol, 36%).

¹H NMR (CD₃OD, 400 MHz): δ 7.67–7.52 (m, 10H); 7.21 (d, *J* = 16.5 Hz, 1H); 7.14 (d, *J* = 2.2 Hz, 2H); 7.07 (dd, *J* = 8.1 Hz, *J* = 1.5 Hz, 1H); 7.02 (d, *J* = 1.6 Hz, 1H). ¹³C NMR (CD₃OD, 100 MHz): δ 156.2; 142.7; 141.9; 138.6; 131.7; 129.2; 127.8; 127.8; 127.5; 127.4; 127.2; 126.9; 126.2; 126.2; 126.1; 126.1; 125.0; 119.5; 114.3. ¹⁹F NMR (CD₃OD, 375 MHz): δ 14.98 (s, 3F); 14.91 (s, 3F). IR (neat): 1611.5; 1428.3; 1319.9; 1163.2; 1107.4; 1066.6; 1014.2; 967.4; 956.5; 872.2; 831.8; 757.9; 750.6; 624.8; 592.8; 507.7.

10.9.1.11. (E,E)-1-Hydroxy-2,5-bis(4-trifluoromethoxy)styrylbenzene (17). Following general procedure **B**, diphosphonate **27** (0.99 g, 1.56 mmol) was reacted with aldehyde **36** (0.74 g, 3.91 mmol). The crude product was purified by column chromatography (0 → 8% EtOAc/light petroleum) and product **17** was obtained as a bright yellow solid (0.47 g, 1.01 mmol, 65%).

¹H NMR (CD₃OD, 400 MHz): δ 7.63 (d, *J* = 5.8 Hz, 2H); 7.61 (d, *J* = 5.6 Hz, 2H); 7.48 (d, *J* = 16.5 Hz, 1H); 7.40–7.34 (m, 1H); 7.27–7.18 (m, 5H); 7.12 (d, *J* = 3.2 Hz, 2H); 7.07 (dd, *J* = 8.1 Hz, *J* = 1.5 Hz, 1H); 7.02 (d, *J* = 1.6 Hz, 1H). ¹³C NMR (CD₃OD, 100 MHz): δ 156.7; 149.7; 149.4; 149.4; 139.2; 139.0; 138.1; 133.0; 130.8; 129.0; 128.8; 128.1; 127.9; 127.7; 126.0; 125.4; 122.3; 122.2; 121.6; 119.7; 114.4. ¹⁹F NMR (CD₃OD, 375 MHz): δ 18.85 (s, 6F). IR (neat): 1604.3; 1557.6; 1515.8; 1505.7; 1269.9; 1158.4; 1099.9; 1015.6; 967.6; 928.0; 839.2; 676.6; 624.0; 525.1.

10.9.1.12. (E,E)-1-Hydroxy-2,5-bis(4-{1,1,2,2-tetrafluoroethyl})styrylbenzene (18). Following general procedure **B**, diphosphonate **27** (0.74 g, 1.17 mmol) was reacted with aldehyde **37** (0.65 g, 2.92 mmol). After work-up, the crude product was subjected to column chromatography (0 → 10% EtOAc/light petroleum) to yield product **18** as a bright yellow solid (0.27 g, 0.5 mmol, 43%).

¹H NMR (CD₃OD, 400 MHz): δ 7.61 (d, *J* = 5.3 Hz, 2H); 7.59 (d, *J* = 5.2 Hz, 2H); 7.56 (d, *J* = 8.1 Hz, 1H); 7.48 (d, *J* = 16.6 Hz, 1H); 7.25–7.19 (m, 5H); 7.12 (d, *J* = 5.5 Hz, 2H); 7.08 (dd, *J* = 7.9 Hz, *J* = 1.7 Hz, 1H); 7.02 (d, *J* = 1.5 Hz, 1H); 6.46–6.14 (m, 2H). ¹³C NMR (CD₃OD, 100 MHz): δ 156.6; 149.2; 139.2; 138.4; 137.6; 130.4; 128.8; 128.6; 128.1; 128.0; 127.9; 125.6; 125.4; 123.0; 123.0; 119.7; 114.3.

10.9.1.13. (E,E)-1-Trifluoromethyl-2,5-bis(4-hydroxy)styrylbenzene (19). Following general procedure **A**, diphosphonate **28** (0.37 g, 0.83 mmol) was reacted with aldehyde **33** (0.49 g, 2.1 mmol). After work-up, the crude product was purified by

column chromatography (0 → 4% EtOAc/light petroleum) and the intermediary bis-TBDMS protected styrylbenzene was obtained as a bright yellow solid (0.36 g, 0.59 mmol, 71%). ¹H NMR (CDCl₃, 400 MHz): δ 7.77–7.72 (m, 2H); 7.61 (d, *J* = 8.1 Hz, 1H); 7.44–7.37 (m, 4H); 7.31 (dd, *J* = 16.1 Hz, *J* = 1.8 Hz, 1H); 7.11 (d, *J* = 16.3 Hz, 1H); 7.05 (d, *J* = 16.0 Hz, 1H); 7.00–6.92 (m, 1H); 6.88–6.81 (m, 4H). ¹³C NMR (CDCl₃, 100 MHz): δ 156.0, 155.9, 136.5, 135.0; 131.7, 130.3, 130.2, 129.6, 129.0, 128.1, 127.9, 126.9, 125.0, 123.8, 122.0, 120.4, 29.7, 25.7, -4.4. ¹⁹F NMR (CDCl₃, 375 MHz): δ 18.17 (s, 3F). IR (neat): 1598.9; 1508.0; 1471.8; 1327.9; 1314.0; 1251.5; 1170.0; 1154.7; 1131.4; 1115.5; 1102.1; 1051.1; 962.1; 938.5; 906.8; 834.5; 778.2; 700.2; 667.7; 660.3; 638.4; 554.5; 534.7.

The bis-TBDMS protected styrylbenzene (0.34 g, 0.54 mmol) was treated with TBAF according to general procedure **C**, and following column chromatography (0 → 30% EtOAc/light petroleum), the impure product was purified by HPLC (CN column, 35:65 → 10:90 of 0.2% aq TFA/MeOH) and product **19** was obtained as a yellow solid (83 mg, 0.22 mmol, 40%).

¹H NMR (CD₃OD, 400 MHz): δ 7.81 (d, *J* = 8.2 Hz, 1H); 7.73 (s, 1H); 7.70 (d, *J* = 8.5 Hz, 1H); 7.42 (d, *J* = 8.0 Hz, 2H); 7.38 (d, *J* = 8.0 Hz, 2H); 7.23 (d, *J* = 16.0 Hz, 1H); 7.14 (t, *J* = 16.9, 2H); 6.99 (d, *J* = 16.3 Hz, 1H); 6.80 (dd, *J* = 7.8 Hz, *J* = 3.5 Hz, 4H).

¹³C NMR (CD₃OD, 100 MHz): δ 159.1; 158.9; 138.3; 136.2; 133.3; 131.1; 130.2; 130.0; 129.3; 129.2; 128.4; 128.0; 127.5; 125.0; 124.9; 124.7; 124.7; 124.6; 124.6; 121.7; 116.7; 116.6. ¹⁹F NMR (CD₃OD, 375 MHz): δ 17.64 (s, 3F). IR (neat): 1605.0; 1512.1; 1441.0; 1313.9; 1257.1; 1239.9; 1199.4; 1171.9; 1153.6; 1108.8; 1079.5; 1049.9; 959.8; 869.9; 837.2; 812.7; 671.7; 552.7; 522.1.

10.9.1.14. (E,E)-1-(2,2,2-Trifluoroethoxy)-2,5-bis(4-hydroxy)styrylbenzene (20). Following general procedure **B**, diphosphonate **29** (0.45 g, 0.95 mmol) was reacted with aldehyde **33** (0.56 g, 2.37 mmol). After work-up, the crude product was subjected to column chromatography (0 → 5% EtOAc/light petroleum) and the bis-TBDMS protected styrylbenzene was obtained as a bright yellow solid (0.4 g, 0.63 mmol, 66%). ¹H NMR (CDCl₃, 400 MHz): δ 7.59–7.51 (m, 4H); 7.43 (d, *J* = 16.5 Hz, 1H); 7.31 (d, *J* = 7.7 Hz, 1H); 7.69 (d, *J* = 8.0 Hz, 1H); 7.24 (d, *J* = 16.4 Hz, 1H); 7.18 (d, *J* = 16.3 Hz, 1H); 7.10–7.06 (m, 2H); 7.00 (dd, *J* = 8.6 Hz, *J* = 2.0 Hz, 4H); 4.56 (q, *J* = 8.2 Hz, *J* = 8.1 Hz, 2H); 1.16 (s, 18H); 0.38 (s, 6H); 0.38 (s, 6H). ¹³C NMR (CDCl₃, 100 MHz): δ 155.6; 155.5; 154.7; 137.9; 131.8; 131.0; 130.3; 129.3; 128.6; 127.7; 126.7; 126.7; 125.8; 121.0; 120.4; 120.3; 120.1; 110.7; 67.2; 66.8; 66.5; 66.1; 29.7; 25.6; -4.4. ¹⁹F NMR (CDCl₃, 375 MHz): δ 3.80 (t, *J* = 8.1 Hz, 3F).

The bis-TBDMS protected styrylbenzene (0.4 g, 0.63 mmol) was treated with TBAF according to general procedure **C**. After work-up, the crude product was purified by column chromatography (0 → 25% EtOAc/light petroleum) and product **20** was obtained as a bright yellow solid (0.127 g, 0.31 mmol, 49%).

¹H NMR (CD₃OD, 400 MHz): δ 7.51 (d, *J* = 8.1 Hz, 1H); 7.40–7.29 (m, 4H); 7.20 (d, *J* = 16.5 Hz, 1H); 7.13 (dd, *J* = 8.1 Hz, *J* = 1.0 Hz, 1H); 7.05 (d, *J* = 16.5 Hz, 1H); 7.03 (d, *J* = 16.3 Hz, 1H); 7.00 (d, *J* = 1.1 Hz, 1H); 6.87 (d, *J* = 16.3 Hz, 1H); 6.81–6.75 (m, 4H); 4.48 (q, *J* = 8.3 Hz, *J* = 8.3 Hz, 2H). ¹³C NMR (CD₃OD, 100 MHz): δ 157.8; 157.6; 155.5; 138.9; 130.4; 130.0; 129.7; 129.5; 128.6; 128.5; 127.2; 125.7; 121.5; 120.0; 116.2; 116.2; 111.4; 67.4; 67.0; 66.7. ¹⁹F NMR (CD₃OD, 375 MHz): δ 6.89 (t, *J* = 7.5 Hz, 3F). IR (neat): 3331.9; 1606.2; 1515.7; 1505.9; 1455.8; 1427.9; 1238.9; 1169.7; 1118.3; 964.1; 828.9; 667.9; 617.9; 518.9.

10.9.1.15. (E,E)-1-(4,4,4-Trifluorobutoxy)-2,5-bis(4-hydroxy)styrylbenzene (21). Following general procedure **B**, diphosphonate **30** (0.50 g, 1 mmol) was reacted with aldehyde **33** (0.59 g,

2.5 mmol). After work-up, the crude product was purified by column chromatography (0 → 2% EtOAc/light petroleum) and the bis-TBDMS protected styrylbenzene was obtained as a bright yellow solid (0.3 g, 0.46 mmol, 46%). ¹H NMR (CDCl₃, 400 MHz): δ 7.53 (d, *J* = 8.1 Hz, 1H); 7.38 (d, *J* = 8.4 Hz, 4H); 7.28 (d, *J* = 16.5 Hz, 1H); 7.12–7.05 (m, 2H); 7.03 (d, *J* = 16.2 Hz, 1H); 6.95 (d, *J* = 1.1 Hz, 1H); 6.92 (d, *J* = 16.3 Hz, 1H); 6.86–6.80 (m, 4H); 4.13 (t, *J* = 6.0 Hz, 2H); 2.46–2.31 (m, 2H); 2.20–2.10 (m, 2H); 0.99 (s, 18H); 0.21 (s, 12H). ¹³C NMR (CDCl₃, 100 MHz): δ 155.9; 155.6; 155.4; 137.9; 131.3; 130.6; 128.7; 128.3; 127.7; 127.6; 126.5; 126.5; 126.1; 120.9; 120.4; 120.3; 119.6; 109.6; 66.6; 31.1; 30.8; 29.4; 25.7; 22.4; 22.3; 18.2; –4.4. ¹⁹F NMR (CDCl₃, 375 MHz): δ 11.39 (t, *J* = 10.9 Hz, 3F). IR (neat): 1599.9; 1508.7; 1471.7; 1250.8; 1166.6; 1153.9; 1027.7; 908.7; 833.2; 798.6; 779.1; 700.5; 661.8; 623.5; 531.4; 504.4.

The silylated bis-styrylbenzene (0.3 g, 0.46 mmol) was deprotected according to general procedure C. After work-up, the crude product was purified using column chromatography (10 → 22.5% EtOAc/light petroleum) and product **21** was obtained as a bright yellow solid (0.12 g, 0.27 mmol, 58%).

¹H NMR (CD₃OD, 400 MHz): δ 7.50 (d, *J* = 8.1 Hz, 1H); 7.38 (d, *J* = 8.6 Hz, 2H); 7.34 (d, *J* = 8.6 Hz, 2H); 7.24 (d, *J* = 16.5 Hz, 1H); 7.11–7.02 (m, 4H); 6.92 (d, *J* = 16.3 Hz, 1H); 6.80–6.75 (m, 4H); 4.13 (t, *J* = 6.0 Hz, 2H); 2.50–2.35 (m, 2H); 2.16–2.06 (m, 2H). ¹³C NMR (CD₃OD, 100 MHz): δ 158.4; 158.2; 157.3; 139.4; 131.1; 130.4; 129.7; 129.5; 128.9; 128.6; 127.3; 127.1; 126.6; 121.1; 120.4; 116.5; 110.8; 67.8; 32.1; 31.8; 31.5; 31.2; 23.5; 23.4; 23.4. ¹⁹F NMR (CD₃OD, 375 MHz): δ 3.48 (t, *J* = 11.3 Hz, 3F). IR (neat): 3325.9; 1605.69; 1593.7; 1515.5; 1505.9; 1447.9; 1385.8; 1338.1; 1241.0; 1171.3; 1026.0; 961.8; 826.7; 621.1; 519.8.

10.9.1.16. (E,E)-1-(Nonafluoro-tert-butoxy)-2,5-bis(4-hydroxy)styrylbenzene (22). Following general procedure B, diphosphate **32** (0.55 g, 0.89 mmol) was reacted with aldehyde **33** (0.53 g, 2.2 mmol). After work-up, the crude product was purified by column chromatography (0 → 2% EtOAc/light petroleum) and the bis-TBDMS protected styrylbenzene was obtained as a bright yellow solid (0.22 g, 0.28 mmol, 32%). ¹H NMR (CDCl₃, 400 MHz): δ 7.27–7.20 (m, 4H); 7.20–7.12 (m, 2H); 6.90–6.81 (m, 2H); 6.79–6.73 (m, 2H); 6.72–6.64 (m, 4H); 7.48 (d, *J* = 8.2 Hz, 1H); 0.84 (s, 1H); 0.06 (s, 6H); 0.06 (s, 6H). ¹³C NMR (CDCl₃, 100 MHz): δ 155.8; 155.8; 150.5; 137.9; 130.5; 130.5; 130.2; 130.0; 129.3; 127.9; 127.8; 126.1; 125.3; 124.2; 120.5; 119.0; 31.9; 29.4; 25.7; –4.4. ¹⁹F NMR (CDCl₃, 375 MHz): δ 8.81 (s, 9F). IR (neat): 1600.0; 1508.4; 1472.0; 1249.8; 1169.5; 1155.1; 1124.8; 998.7; 965.7; 904.5; 833.8; 779.5; 726.0; 700.6; 537.4; 504.5. The bis-TBDMS protected styrylbenzene was treated with TBAF according to general procedure C. The crude product was subjected to column chromatography (10 → 25% EtOAc/light petroleum) and product **22** was obtained as a bright yellow solid (72 mg, 0.13 mmol, 47%).

¹H NMR (CD₃OD, 400 MHz): δ 7.72 (d, *J* = 8.3 Hz, 1H); 7.46–7.34 (m, 5H); 7.31 (s, 1H); 7.22 (d, *J* = 16.5 Hz, 1H); 7.05 (d, *J* = 16.4 Hz, 1H); 7.10 (d, *J* = 12.4 Hz, 1H); 6.96–6.90 (m, 1H); 6.82–6.77 (m, 4H). ¹³C NMR (CD₃OD, 100 MHz): δ 159.0; 158.9; 151.6; 139.6; 131.8; 131.7; 130.9; 130.1; 129.9; 129.3; 129.1; 127.4; 125.5; 125.1; 123.0; 120.1; 119.8; 118.7; 116.7; 116.6. ¹⁹F NMR (CD₃OD, 375 MHz): δ 10.93 (s, 9F). IR (neat): 3332.1; 1606.3; 1515.6; 1250.3; 1171.8; 1123.0; 1000.3; 965.1; 829.3; 727.4; 668.0; 529.1.

10.9.1.17. (E,E)-1-Hydroxy-2,5-bis(3-trifluoromethyl-4-methoxy)styrylbenzene (23). Following general procedure B, diphosphate **27** (0.52 g, 1 mmol) was reacted with aldehyde **38** (0.51 g, 2.5 mmol). After work-up, the crude product was purified by column chromatography (0 → 17% EtOAc/light petroleum), followed by preparative TLC (eluent: 50% EtOAc/light petroleum) and product **23** was obtained as a bright yellow solid (58 mg, 0.12 mmol, 12%).

¹H NMR (acetone-*d*₆, 400 MHz): δ 7.80–7.71 (m, 4H); 7.54 (d, *J* = 8.0 Hz, 1H); 7.39 (d, *J* = 16.6 Hz, 1H); 7.26–7.16 (m, 3H); 7.13 (d, *J* = 16.4 Hz, 1H); 7.10–6.98 (m, 3H); 3.90 (s, 6H). ¹³C NMR (acetone-*d*₆, 100 MHz): δ 156.2; 139.0; 132.5; 132.2; 131.9; 131.1; 129.0; 127.8; 127.6; 127.4; 125.8; 125.7; 125.6; 125.5; 125.0; 124.1; 119.3; 114.3; 113.9; 56.6; 56.6. ¹⁹F NMR (acetone-*d*₆, 375 MHz): δ 7.62 (s, 3F); 7.60 (s, 3F). IR (neat): 3523.0; 1615.5; 1512.0; 1501.5; 1428.0; 1327.6; 1274.3; 1261.6; 1119.8; 1058.0; 1017.1; 963.1; 823.7; 667.6; 645.9; 569.8; 544.1.

10.9.1.18. (E,E)-1-Methoxy-2,5-bis(3-trifluoromethyl-4-methoxy)styrylbenzene (24). Following general procedure B, diphosphate **25** (0.41 g, 1 mmol) was reacted with aldehyde **38** (0.51 g, 2.5 mmol). After work-up, the crude product was purified by column chromatography (0 → 10% EtOAc/light petroleum) and product **24** was obtained as a bright yellow solid (0.14 g, 0.27 mmol, 27%).

¹H NMR (DMSO-*d*₆, 400 MHz): δ 7.97–7.83 (m, 3H); 7.81 (dd, *J* = 7.8 Hz, *J* = 1.7 Hz, 1H); 7.76 (d, *J* = 1.7 Hz, 1H); 7.65 (d, *J* = 8.1 Hz, 1H); 7.46 (d, *J* = 16.8 Hz, 1H); 7.40–7.20 (m, 6H); 3.93 (s, 3H); 3.92 (s, 3H). ¹³C NMR (DMSO-*d*₆, 100 MHz): δ 156.1; 137.9; 131.8; 131.5; 130.0; 129.7; 129.2; 128.8; 127.8; 127.3; 127.0; 126.6; 125.6; 125.1; 122.4; 122.2; 120.7; 119.3; 117.5; 117.2; 114.6; 113.4; 109.1; 56.3; 56.2.

¹⁹F NMR (DMSO-*d*₆, 375 MHz): δ 17.26 (s, 3F); 17.2 (s, 3F). IR (neat): 1615.6; 1510.4; 1505.8; 1463.9; 1328.5; 1260.0; 1118.3; 1054.9; 1021.0; 959.3; 818.0; 667.8; 645.5; 541.1.

Acknowledgments

This research was performed within the framework of CTMM, the Center for Translational Molecular Medicine (www.ctmm.nl), project LeARN (grant 02N-101).

Supplementary data

Supplementary data associated with this article can be found in the online version, at <http://dx.doi.org/10.1016/j.bmc.2014.02.054>.

Reference and notes

- Duyckaerts, C.; Delatour, B.; Potier, M. C. *Acta Neuropathol.* **2009**, *118*, 5.
- Frisoni, G. B.; Fox, N. C.; Jack, C. R., Jr.; Scheltens, P.; Thompson, P. M. *Nat. Rev. Neurol.* **2010**, *6*, 67.
- Jack, C. R., Jr.; Knopman, D. S.; Jagust, W. J.; Shaw, L. M.; Aisen, P. S.; Weiner, M. W.; Petersen, R. C.; Trojanowski, J. Q. *Lancet Neurol.* **2010**, *9*, 119.
- Vandenberghe, R.; Van, L. K.; Ivanoiu, A.; Salmon, E.; Bastin, C.; Triau, E.; Hasselbalch, S.; Law, I.; Andersen, A.; Korner, A.; Minthon, L.; Garraux, G.; Nelissen, N.; Bormans, G.; Buckley, C.; Owenius, R.; Thurfjell, L.; Farrar, G.; Brooks, D. J. *Ann. Neurol.* **2010**, *68*, 319.
- Barthel, H.; Gertz, H. J.; Dresel, S.; Peters, O.; Bartenstein, P.; Buerger, K.; Hiemeyer, F.; Wittemer-Rump, S. M.; Seibyl, J.; Reiningner, C.; Sabri, O. *Lancet Neurol.* **2011**, *10*, 424.
- U.S. Food and Drug Administration, *J. Nucl. Med.* **2013**, *54*, 10N.
- Yang, L.; Rieves, D.; Ganley, C. N. *Engl. J. Med.* **2012**, *367*, 885.
- Styren, S. D.; Hamilton, R. L.; Styren, G. C.; Klunk, W. E. *J. Histochem. Cytochem.* **2000**, *48*, 1223.
- Zhuang, Z. P.; Kung, M. P.; Hou, C.; Skovronsky, D. M.; Gur, T. L.; Plossl, K.; Trojanowski, J. Q.; Lee, V. M.; Kung, H. F. *J. Med. Chem.* **2001**, *44*, 1905.
- Klunk, W. E.; Bacskai, B. J.; Mathis, C. A.; Kajdasz, S. T.; McLellan, M. E.; Froesch, M. P.; Debnath, M. L.; Holt, D. P.; Wang, Y.; Hyman, B. T. *J. Neuropathol. Exp. Neurol.* **2002**, *61*, 797.
- Higuchi, M.; Iwata, N.; Matsuba, Y.; Sato, K.; Sasamoto, K.; Saido, T. C. *Nat. Neurosci.* **2005**, *8*, 527.
- Flaherty, D. P.; Walsh, S. M.; Kiyota, T.; Dong, Y.; Ikezu, T.; Vennerstrom, J. L. *J. Med. Chem.* **2007**, *50*, 4986.
- Amatsubo, T.; Morikawa, S.; Inubushi, T.; Urushitani, M.; Taguchi, H.; Shirai, N.; Hirao, K.; Kato, M.; Morino, K.; Kimura, H.; Nakano, I.; Yoshida, C.; Okada, T.; Sano, M.; Tooyama, I. *Neurosci. Res.* **2009**, *63*, 76.
- Bacskai, B. J.; Hickey, G. A.; Skoch, J.; Kajdasz, S. T.; Wang, Y.; Huang, G. F.; Mathis, C. A.; Klunk, W. E.; Hyman, B. T. *Proc. Natl. Acad. Sci. U.S.A.* **2003**, *100*, 12462.
- Bolander, A.; Kieser, D.; Scholz, C.; Heyny-von, H. R.; Mall, G.; Goetschy, V.; Czech, C.; Schmidt, B. *Neurodegener. Dis.* **2013**.

16. Saroja, G.; Soujanya, T.; Ramachandram, B.; Samanta, A. *J. Fluoresc.* **1998**, *8*, 405.
17. Raymond, S. B.; Skoch, J.; Hills, I. D.; Nesterov, E. E.; Swager, T. M.; Bacskai, B. J. *Eur. J. Nucl. Med. Mol. Imaging* **2008**, *35*, S93.
18. Ran, C.; Xu, X.; Raymond, S. B.; Ferrara, B. J.; Neal, K.; Bacskai, B. J.; Medarova, Z.; Moore, A. *J. Am. Chem. Soc.* **2009**, *131*, 15257.
19. Lockhart, A.; Ye, L.; Judd, D. B.; Merritt, A. T.; Lowe, P. N.; Morgenstern, J. L.; Hong, G.; Gee, A. D.; Brown, J. *J. Biol. Chem.* **2005**, *280*, 7677.
20. Meadowcroft, M. D.; Connor, J. R.; Smith, M. B.; Yang, Q. X. *J. Magn. Reson. Imaging* **2009**, *29*, 997.
21. Buell, A. K.; Esbjorner, E. K.; Riss, P. J.; White, D. A.; Aigbirhio, F. I.; Toth, G.; Welland, M. E.; Dobson, C. M.; Knowles, T. P. *Phys. Chem. Chem. Phys.* **2011**, *13*, 20044.
22. Pike, V. W. *Trends Pharmacol. Sci.* **2009**, *30*, 431.
23. Benhaim, D.; Grushka, E. *J. Chromatogr. A* **2008**, *1209*, 111.
24. Lombardo, F.; Shalaeva, M. Y.; Tupper, K. A.; Gao, F.; Abraham, M. H. *J. Med. Chem.* **2000**, *43*, 2922.
25. Lombardo, F.; Shalaeva, M. Y.; Tupper, K. A.; Gao, F. *J. Med. Chem.* **2001**, *44*, 2490.
26. Yanagisawa, D.; Taguchi, H.; Ibrahim, N. F.; Morikawa, S.; Shiino, A.; Inubushi, T.; Hirao, K.; Shirai, N.; Sogabe, T.; Tooyama, I. *J. Alzheimers Dis.* **2014**, *39*, 617.
27. Brooks, A. F.; Rodnick, M. E.; Fawaz, M. V.; Desmond, T. J.; Scott, P. J. *J. Labelled Compd. Radiopharm.* **2013**, *56*, S29.
28. van der Born, D.; Herscheid, J. D. M.; Vught, D. J. *J. Labelled Compd. Radiopharm.* **2013**, *56*, S1.